

STABILITY AND NANOSTRUCURE OF HETEROGENEOUS AMORPHOUS SILICON THIN-FILM SYNTHESIZED UNDER HIGH CHAMBER PRESSURE (500 TO 2200 mTorr) REGIME OF RF PECVD

A. R. MIDDYA^{1,2a}, S. HAMMA^{1b}, S. HAZRA^{2c}, S. RAY² AND C. LONGEAUD³

¹Laboratoire de Physique des Interfaces et des Couches Minces (UMR 7647 CNRS), Ecole Polytechnique, 91128 Palaiseau, Cedex, FRANCE; ²Energy Research Unit, Indian Association for the Cultivation of Science, Jadavpur, Calcutta - 70 032, INDIA; ³Laboratoire de Genie Electrique de Paris (CNRS, URA 0127), Ecole Superieure d'Electricite, Universites Paris VI et Paris XI, Plateau de Moulon 91192 Gif-Sur-Yvette, Cedex, FRANCE

ABSTRACT

We report on improvement in stability of a new type of amorphous silicon films, synthesized (*growth rate* > 0.1 nm/s) by driving the plasma condition close to the *powder regime* (or “ γ -regime”) of rf PECVD. These films exhibit high mobility-lifetime products [$(\mu\tau)_{\text{annld}} \sim 10^{-4}$ cm²/V, $\sigma_{\text{ph}}/\sigma_{\text{d}} \sim 5\text{-}10 \times 10^5$, $E_{\text{a}} \approx 0.7 - 0.9$ eV], compact network structure [$C_{\text{H}} \approx 7$ to 8 at%, nanovoid density < 0.01 %, $\rho \approx 2.23 \pm 0.01$ gm/cm³], new features of optical properties and density-of-state (DOS) above E_{F} is significantly lower than that of state-of-the art films. The kinetics of light-induced (AM 1.5) degradation of $\mu\tau$ is very fast and *saturated* $\mu\tau \sim 10^{-6}$ cm²/V, *a value similar to that of conventional a-Si:H films at annealed state*. The improved stability of “new” a-Si films, henceforth it will be denoted as “**quasi-amorphous silicon (qm-Si) thin-film**”, will be correlated with its specific nanostructure.

INTRODUCTION

The improved stability of high H-diluted a-Si:H materials or protocrystalline Si films compared to undiluted films convincingly demonstrates that microstructure of Si-Si network influences in a complex way defect creation process during light-soaking [1, 2, 3]. In other words, light-induced degradation (LID) is sensitivite to the details of Si-Si tetrahedral network structure, local small-scale ordering in addition to bonded hydrogen content and concentration of polyhydride bonds [(SiH₂)_n]. In this work, we report on another experimental evidence that how Si-Si network structure in amorphous matrix is important in determining LID metastability of a-Si:H films. These ‘new’ type of amorphous silicon thin-film have been developed by running the plasma condition close to powder regime (γ -regime) of radio frequency plasma-enhanced chemical vapor deposition (rf PECVD) which exhibit significantly improved stability compared to state-of-the-art a-Si:H films [4, 5, 6]. These films are amorphous and do not exhibit thickness dependence phase transition (as it happens in high H-diluted films), however complimentary str-

Present address: a. Department of Physics, Syracuse University, Syracuse, NY 13244-1130, b. Novellus Systems, Inc., San Jose, CA 95134, c. Institute of Energy Conversion, University of Delaware, Newark, DE 19716-3820.

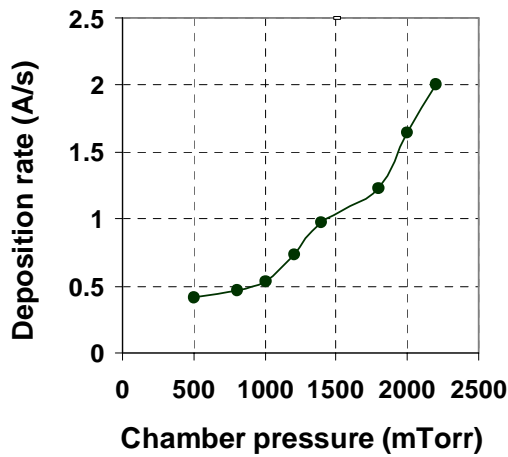


Fig. 1: Variation of deposition rate with chamber pressure.

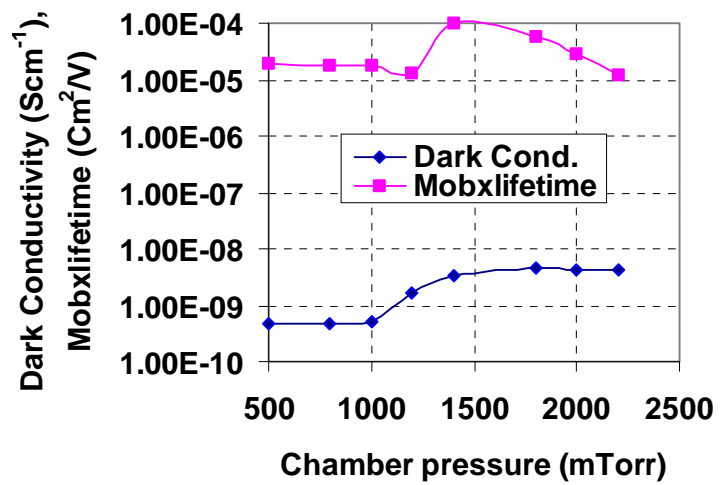


Fig. 2: Variation of dark conductivity & mobility-lifetime product with chamber pressure.

uctural characterization technique reveals its nanostructure, which is different from conventional a-Si:H films. In this work we shall illustrate how initial electronic properties and light-induced degradation of a-Si:H can be improved by controlling its atomic-scale structure or nanostructure.

EXPERIMENTAL DETAILS

The films for this study have been prepared by radio frequency (13.56 MHz) plasma-enhanced chemical vapor deposition (rf PECVD). The ratio of silane (SiH_4) to helium (He) was maintained such that the deposition rate was close to 1 A/s or higher. The chamber pressure (P_r) was varied from 500 to 2200 mTorr to run the plasma close to powder formation regime. The plasma power and substrate temperature have been maintained at 15 mW/cm² and 210°C respectively. The photoconductivity of qm-Si:H has been measured under 50 mW/cm² white light and the mobility-lifetime product ($\mu\tau$) has been estimated from D.C. photoconductivity measured under 700 nm (through interference filter) illumination with a generation rate of $3 \times 10^{18} \text{ cm}^{-3} \text{ s}^{-1}$. The density-of-state of the samples has been studied by modulated photocurrent experiments (MPC). Extensive characterization of Si-Si and Si-H network structure have been carried out using infrared Fourier transform spectroscopy (FTIR), Raman Spectroscopy, UV-VIS ellipsometry, SAXS, XRD and floatation density method. The light soaking study has been done under 100 mW/cm² white light through IR filter. The temperature of the sample during light soaking has been maintained at 45 - 50°C by air cooling.

RESULTS AND DISCUSSION

Fig.1 shows the variation of deposition rate (R_d) with chamber pressure (P_r) during film growth. The values of R_d remain almost constant at 0.5 A/s with increasing P_r from 500 to 1000 mTorr, however R_d suddenly enhanced by a factor of 2 (≈ 1 A/s) as P_r increases to 1400 mTorr after that it increases monotonically with P_r . This sudden increase of R_d is a signature of transition from α - to γ -regime, to be precise γ' -regime of rf PECVD [8]. With change of plasma regime the mechanism of energy transfer mechanism via electron from plasma (rf generator) to the gas precursors changes during the process of electrical discharge of silane and helium mixture [9].

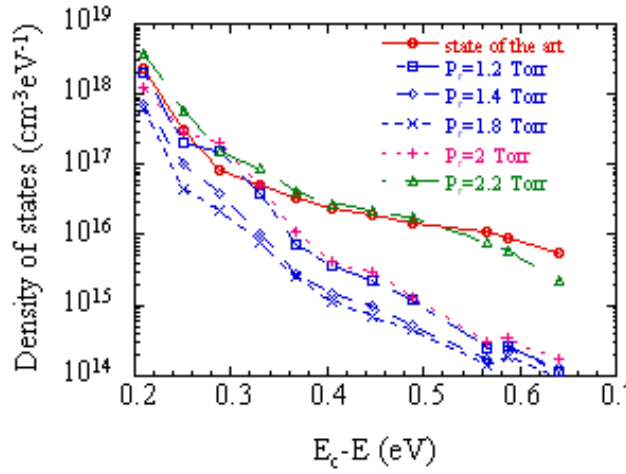


Fig. 3: Variation of MPC-DOS with chamber pressure.

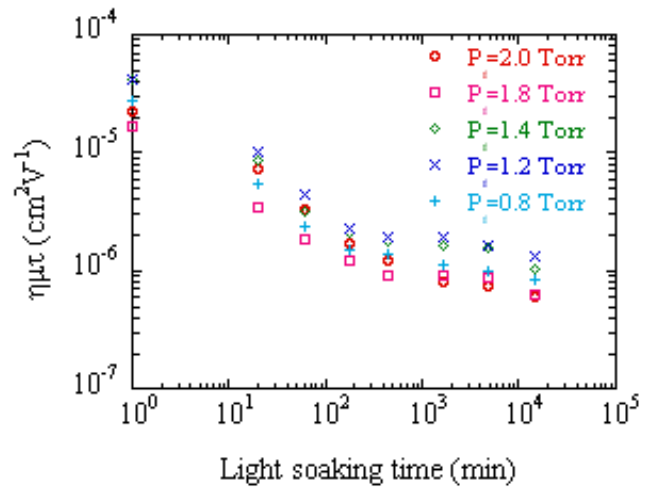


Fig. 3: Light-induced degradation kinetics of mobility-lifetime product qm-Si films

The transition of plasma regime is also corroborated by the sudden (as expected) change in the electronic properties of the resulting films at or greater than 1000 mTorr as shown in Fig. 2(b) & 3. The effect of chamber pressure (transition of plasma regime from α - to γ) on electronic properties and stability of a-Si:H films has also been reproduced in another reactor at Ecole Polytechnique, where similar variation (factor of 2 to 3) of R_d accompanied by sudden increase of peak-to-peak voltage at the powered electrode have been observed with chamber pressure [10]. Phillips, UK also reported transition of plasma regime (α - to γ -regime) of rf PECVD accompanied by a sudden increase of R_d by a factor of 2 to 3 [11]. Fig. 2 displays the variation of electronic properties of the films with chamber pressure (P_r), i.e. transition of plasma regime (α - to γ). The electron mobility lifetime product ($\mu\tau$) increases from 10^{-5} cm²/V to 10^{-4} cm²/V as P_r increases from 1000 to 1400 mTorr. The dark conductivity (σ_d) remain almost constant (10^{-10} S/cm) as P_r increases from 500 to 1000 mTorr, however it suddenly increases to 10^{-9} S/cm as P_r exceeds 1000 mTorr. The dark conductivity activation energy varies 0.9 to 0.7 eV as σ_d increases from 10^{-10} to 10^{-9} S/cm. The transmission measurement reveals a small reduction of optical gap, which may cause increase of σ_d ($n \sim e^{-E_g/KT}$). The improvement of $\mu\tau$ can not be attributed to the simple movement of Fermi level towards conduction band (E_C) since simultaneously hole diffusion length (L_D) also increases with chamber pressure (P_r). The value of L_D increases by 54%, as P_r is varied 500 to 1800 mTorr. The improvement in electronic properties for $P_r > 1000$ mTorr should have reflection in the density-of-state (DOS) of the films. In Fig. 3 the DOS above E_F estimated from Modulated Photocurrent experiment (MPC) at annealed state of the samples has been plotted versus chamber pressure (P_r). In the same plot MPC-DOS of a standard sample is also shown. It may be noted from the figure that MPC-DOS above E_F systematically decreases as P_r increases from 500 to 1800 mTorr, then DOS starts increasing again for $P_r > 1800$ mTorr. MPC-DOS as low as 5×10^{14} cm⁻³eV⁻¹ for $E_C - E_F \approx 0.5$ eV has been observed for samples prepared with $P_r \approx 1800$ mTorr. This is the lowest reported DOS at $E_C - E_F \approx 0.5$ eV for a-Si:H films. The kinetics of light-induced degradation of $\mu\tau$ of these films, as shown in Fig. 4. The values of $\mu\tau$ of qm-Si films degrade *very fast* and tend to saturate at $\mu\tau \sim 10^{-6}$ cm²/V. The saturation occurs in the time scale of 20 to 30 hrs compared to more than 600 hrs for standard H-diluted samples. Thus, not only kinetics is very fast but also saturated values of $\mu\tau$ of qm-Si:H films is similar to that of conventional a-Si:H at annealed state. The improved stability is most likely related to its microstructure. The FTIR measurement show that qm-Si films have much lo-

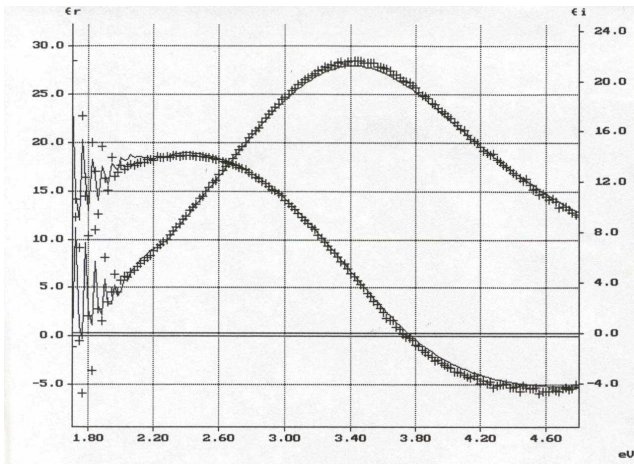


Fig. 4a: Experimental and simulated data of spectral dependence of dielectric function (ϵ_1 & ϵ_2) of sample P2 (1000 mT).

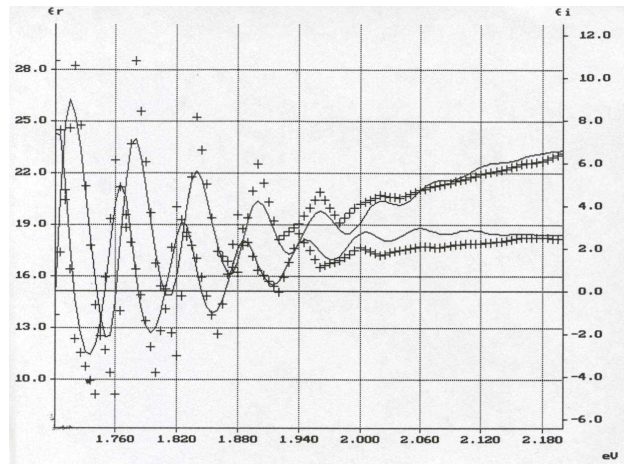


Fig. 4b: Experimental and simulated data of dielectric function (ϵ_1 & ϵ_2) versus photon energy (< 1.8 eV) of sample P2.

wer bonded H-content (6 to 8 at%) compared to that (12 to 15 at%) of standard a-Si:H and Si-H bond of qm-Si films appears at 2010 cm^{-1} instead of 2000 cm^{-1} [4]. The new features of the network structure in qm-Si films is also observed in optical transmission measurement, the $(\alpha h\nu)^{1/2}$ vs. $h\nu$ curve (Tau's plot) for this series of samples is not a straight-line, rather data of $(\alpha h\nu)^{1/3}$ vs. $h\nu$ plot appear in straight-line indicating subtle difference in the optical properties of qm-Si films compared to conventional a-Si:H films. The spectral dependence of dielectric function of qm-Si films (measured by UV-VIS ellipsometry) exhibit characteristic

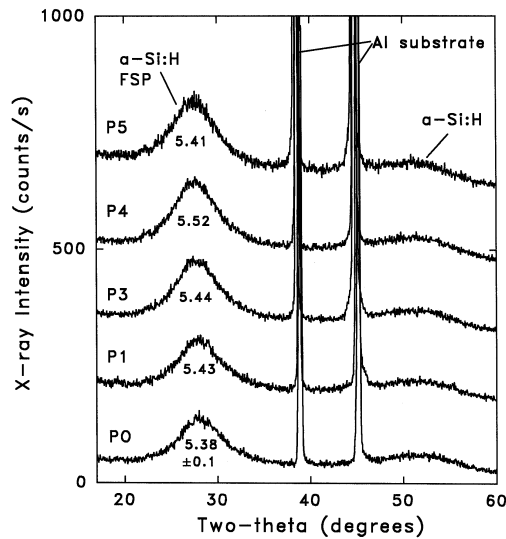


Fig. 5: X-ray diffraction of samples prepared with different chamber pressure.

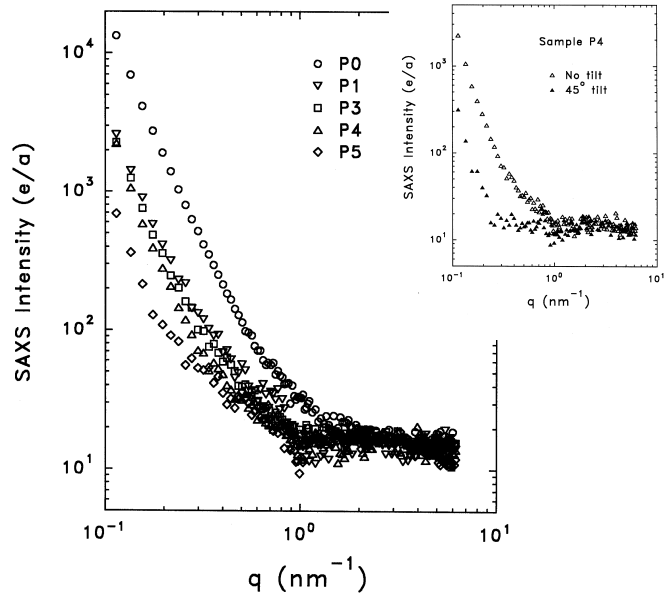


Fig. 6: Comparison of SAXS signal of qm-Si films prepared with different chamber pressure. Inset figure shows effect of 45-degree tilt on SAXS signal of P4 sample.

peak at 3.5 eV with no signature of peak at 4.2 eV (corresponds to c-Si). We studied samples having thickness ranging from 0.5 to 2.5 μm on glass substrates, in all cases we observed one peak at 3.5 eV, i.e. there is no thickness dependence phase transition ($a \rightarrow \mu\text{c}$) *which is a characteristic feature of high H-diluted films or protocrystalline silicon thin-film* [11]. Thus even thick film (2 - 4 μm) qm-Si film is amorphous-like. The detailed analysis of ellipsometric spectra provides further insight about the optical properties of qm-Si films. Fig. 4a shows a typical variation (experimental) of the dielectric function of qm-Si films (P2) with photon energy. Assuming effective-medium (E-M) theory (a-Si:H is composed of a-Si and void), the experimental data of Fig. 4a can not be simulated as routinely done for conventional a-Si:H. However when a crystalline silicon component is introduced in addition to a-Si and void in the first 175 nm layer (total thickness ≈ 417 nm), then the simulated curve exactly reproduced experimental data even interference fringes at the low energy portion of the spectrum as shown in Fig. 4a & 4b. In other words, to reproduce the experimental data, an adhoc assumption is required that initial half of the film thickness contains crystallites which physically sounds puzzling since the presence of crystalline phase in these materials could not be proved convincingly by any standard techniques. In this situation, we can only comment that *optical properties of qm-Si:H is different from conventional a-Si:H films*.

Fig 5 displays the XRD pattern of qm-Si:H films deposited with different chamber pressure (P_r). The XRD pattern shows that all the samples are amorphous and the full-width-half-maximum (FWHM) of the first scattering peak (FSP) remain almost same (5.4 ± 0.1 degrees) irrespective of chamber pressure. It should be mentioned that there is additional line broadening (FWHM) due to Al-substrates, i.e. FWHM of FSP of all samples would be lower if the samples were on glass substrates. Even FWHM of FSP of qm-Si:H films on Al-substrate is comparable to that of high H-diluted materials of USSC and hot-wire CVD films of NREL [12]. The improved electronic properties, stability ($\mu\tau \sim 10^{-6} \text{ cm}^2/\text{V}$) and DOS above E_F of qm-Si films are possibly linked with the improvement of its tetrahedral Si-Si network structure as evidenced from narrow FSP and nanocrystalline-like optical properties. Further evidence on nanostructural improvement of qm-Si has been obtained from SAXS and floatation density measurements. Fig. 6 shows the variation of SAXS signal with scattering angle ($q=2\pi\theta/\lambda$) for qm-Si samples prepared with different chamber pressure. The SAXS intensity for all samples is very weak above $q = 1 \text{ nm}^{-1}$ and is independent of q in this range. However there are step rise at low q as characterize by the “A” parameter (coefficient of q^{-3} term) [12], indicating different amounts of some large-scale microstructure ($> 20 \text{ nm}$). This large-scale structure has some orientation since “A” parameter decreases significantly upon tilting to 45° at low q (sample P4) as shown in the inset of Fig. 6. The large-scale feature systematically decrease with increasing chamber pressure, indicating homogeneity in the film improves with increasing P_r . For all samples there is no detectable nanostructural SAXS (I_N), so the integrated intensity due to such features (Q_N) is estimated to be less than 2 E22 eu/cm^3 which corresponds to 0.01 vol% nanovoids (detection limit). The mechanical density (ρ) for all the samples (P0 to P5) is nearly constant at $2.23 \pm 0.01 \text{ gm/cm}^3$ consistent with no difference in nanovoid fractions among the samples. The value of Q_N even for sample P0 (500 mTorr) is similar to high H-diluted a-Si:H of USSC samples, SAXS signal is only due to large-scale structure [12], so Q_N of higher chamber pressure ($> 1000 \text{ mTor}$) sample is expected to be still lower. Therefore the improved stability [$(\mu\tau)_{ss} \sim 10^{-6} \text{ cm}^2/\text{V}$], *fast kinetics of degradation* and significantly lower DOS above E_F , all are as a result of improved local ordering in Si-Si network structure (low FSP) and reduction of macroscopic defects of qm-Si films.

CONCLUSIONS

We demonstrated that amorphous silicon thin-film synthesized by running the plasma close to powder regime ($P_r \approx 500$ to 2200 mTorr) of rf PECVD (called “ γ -regime”) exhibits high initial (10^{-4} cm²/V) and stabilized (10^{-6} cm²/V) mobility-lifetime products and very fast kinetics of light-induced degradation. It is a second generation of amorphous silicon thin-film and we call it “**quasi-amorphous silicon (qm-Si) thin-film**”. The optical properties of qm-Si are different from that of conventional a-Si:H films. The lower DOS above E_F and improved metastability and fast kinetics of qm-Si:H films possibly linked with its improved local ordering of Si-Si tetrahedral network structure and low nanostructural defects as evidenced by XRD and SAXS. *The advantage of qm-Si films over high H-diluted or protocrystalline silicon thin films is that the growth rate of qm-Si films is 1 Å/s or more and it be increased even higher.*

ACKNOWLEDGEMENTS

We are grateful to Professor A. K. Barua of IACS, India and Dr. Jerome Perrin of Air-Liquide, France for many interesting discussions and valuable insights. We would like to thank Prof. D. L. Williamson of Colorado School of Mines, CO, USA for XRD and SAXS measurements. This work has been carried out under projects funded by Ministry of Non-Conventional Energy (MNES), India the United Nation Development Program (UNDP, Vienna, Austria) at IACS, Calcutta and also under Indo-French Center for the Promotion of Advance Research.

REFERENCES

1. D. V. Tsu, B. S. Chao, S. R. Ovshinsky, S. Guha and J. Yang, Appl. Phys. Lett. 71 (1997) 1317.
2. J. Koh, Y. Lee, H. Fujiwara, C. R. Wronski and R. W. Collins, Appl. Phys. Lett. 73 (1998) 1526.
3. Y. Zhao, G. Kong, G. Pan, X. Liao, Phys. Rev. Lett. 74 (1995) 558.
4. S. Ray, S. Hazra, A. R. Middy and A. K. Barua, Conf. Record. 1st World PVSC conference, (Hawaii, 1994) 551.
5. A. R. Middy, S. Hazra, S. Ray, C. Longeaud and J. P. Kleider, Mat. Res. Soc. Symp. Proc. 467 (1997) 615.
6. S. Hazra, A. R. Middy, C. Longeaud and S. Ray, Appl. Phys. Letts. 76 (2000) 2340.
8. J. Perrin, Plasma Deposition of Amorphous-based Materials edited by G. Bruno, P. Capezzuto and A. Madan (Academic Press, 1995) p. 216; J. Perrin, J. Non-Cryst. Solids 137 & 138 (1991) 639.
9. P. Roca i Cabarrocas, S. Hamma, S. N. Sharma, G. Viera, E. Bertran and J. Costa, J. Non-Cryst. Solids 227-230 (1998) 871.
10. I. D. French, S. C. Deane, D. T. Murley, J. Hewett, I. G. Gale and M. J. Powell, Mat. Res. Soc. Symp. Proc. 467 (1997) 875.
11. A. S. Ferlauto, J. Koh, P. I. Rovira, C. R. Wronski and R. W. Collins, Mat. Res. Soc. Symp. Proc. 557 (1999) 579.
12. D. L. Williamson, Mat. Res. Soc. Symp. Proc. 377 (1995) 251, D. L. Williamson, Mat. Res. Soc. Symp. Proc. 557 (1999) 251.